Investigation of the anomalous polarimetric signature of a mountainous convective event.

by Jacopo Grazioli and Alexis Berne

Laboratoire de Télédétection Environnementale (LTE)
École Polytechnique Fédérale de Lausanne (EPFL), Switzerland

Abstract

A case study of an intense convective event occurring in the Swiss Alps (Davos) is presented. Polarimetric X-band observations of this event showed an unusual strong signature in terms of differential reflectivity Z_{dr}, differential phase shift on backscattering δ, and correlation coefficient ρ_{hv}. The nature of the event is investigated as well as the possible microphysical processes that may lead to high values of δ and Z_{dr} at X-band. In addition, the consistency between the polarimetric radar variables is experimentally studied.

1 Introduction

On the 12th of July 2010, in the late afternoon, an intense convective event affected the area around the city of Davos (CH). A dual-polarization X-band Doppler radar (MXPol) and three Parsivel disdrometers, belonging to the Environmental Remote Sensing Laboratory (LTE, being the French acronym) of the École Polytechnique Fédérale de Lausanne (EPFL) recorded the evolution of this convective event.

In the most intense part, precipitation was organized in small cells with a core characterized by high values of reflectivity Z_h (50-55 dBZ) and differential reflectivity Z_{dr} (4-6 dB). In RHI scans, their vertical structure emerges as columns of positive Z_{dr}, similar to what has been described in observations at S-band by Hall et al. (1984) and Bringi and Chandrasekar (2001). In these areas, profiles of total differential phase shift Ψ_{dp} exhibit enhanced positive bumps (up to 20-25 °), due to the differential phase shift on backscattering (δ). The copolar correlation coefficient ρ_{hv} tends to decrease, even below 0.95. High values of δ and Z_{dr} (up to 6 dB) attracted our attention to the exceptionality of the event and we investigate which microphysical processes could lead to these particular signatures.

In rain, positive values of Z_{dr} and δ are associated with the presence in the radar sampling volume of oblate and therefore large particles (e.g., Beard et al., 2010). Even a small number of such particles can have a significant influence on this polarimetric observables. The decrease in ρ_{hv} in turns, can be associated with a large width in the drop size distribution (Thurai et al., 2008), when such particles are present.

In particular cases, the presence of positive Z_{dr} can also be related to oblate hail as described by Smyth et al. (1999). Furthermore, computational studies (Aydin and Zhao, 1990) suggest that melting hail may lead to positive δ and in some cases to consistent decreases in correlation coefficient ρ_{hv}. Hail is usually assumed to be tumbling while falling, leading to Z_{dr} values close to 0, in areas of high Z_h (Depue et al., 2007). Positive Z_{dr} values represents therefore a departure from this behaviour.

Thus, the case under investigation may have multiple interpretations, and it presents unusual high values of some polarimetric variables (Z_{dr} and δ) which are peculiar in any scenario proposed.

2 Convective event description

2.1 Event evolution

The convective event of interest started to be evident in the radar images around 1750 UTC on July 12th, 2010. Convective cells with approximate width of 2-3 km are visible in the PPIs from 1750 UTC to 19 UTC (Figure 1). Later, a stratiform configuration became evident, with a clear bright band situated approximately 2 km above the radar altitude. In the convective part of the event, the cells moved from South-West to North-East, following the direction of the valley below, oriented South to North and covered by an RHI scan (Figure 2).

2.2 Data processing

The data recorded by MXPol were aquired in Dual Pulse Pair mode, using 70 pulses at each range gate. The antenna half-power beamwidth is 1.45°, and the range gate resolution employed is 75 m. Clutter filtering was automated in the software using Doppler velocity, and a clutter filter width of 0.37 ms^{-1} was the result of pulse repetition times of 950 and 1200 μs, and 14 clutter averaging intervals. With a rotational speed of 6 ° s^{-1} the obtained angular resolution was about 1°.

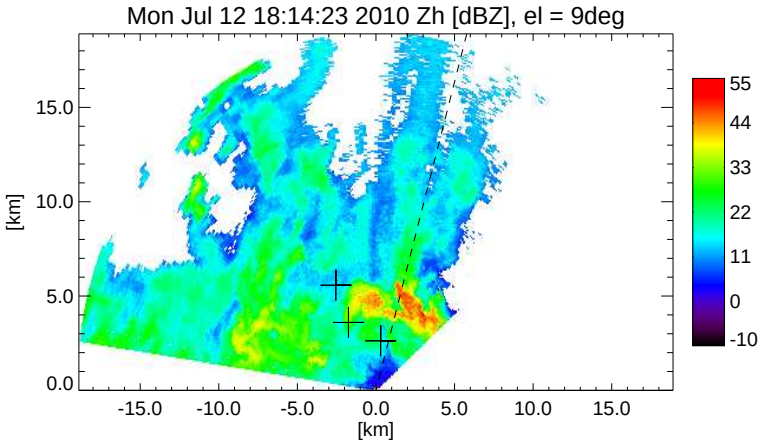

Figure 1: *PPI of Z_h (1814 UTC) at an elevation angle of 9°. The crosses indicate the positions of the three Parsivel disdrometers and the dotted line indicates the direction of the RHI scan.*

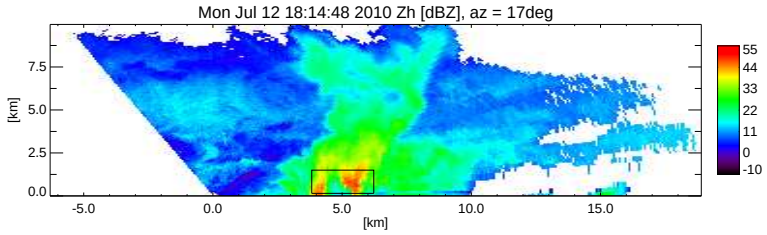

Figure 2: *RHI of Z_h (1814 UTC) along an azimuth of 22° N-E. The box encloses the most intense cells, below the estimated height of the melting layer.*

The areas where the Signal to Noise Ratio (SNR) was below 5 dB were removed from the following analysis, and they are evident at the edges of the intense cells (Figure 1). Attenuation correction for Z_h and Z_{dr} has been performed using the ZPHI method of Testud et al. (2000), parameterized using simulated DSD fields (Schleiss et al., 2012) that are considered as representative of the climatology of Switzerland. The differential phase shift on propagation Φ_{dp}, necessary input of the method, has been calculated by iterative filtering of Ψ_{dp} profiles, following the procedure proposed by Hubbert and Bringi (1995) and further developed by Wang and Chandrasekar (2009). At the time of the event, the radar did not include a calibration sequence for Z_{dr}, and in order to verify any possible miscalibration, the vertical profiles of the RHI scans were used, as we expect an average value of 0 dB in that direction. In the present case, no significant bias was detected.

2.3 Polarimetric signatures

As introduced before, the polarimetric signature of the event under consideration was significant. The cells, moving from South-East to North-West are characterized by cores of high reflectivity Z_h, with maximum values around 50-55 dB (Figures1 and 2) and correspondingly, values of differential reflectivity Z_{dr} constantly above 4 dB with some peaks above 6 dB (Figures 3 and 4).

Among the polarimetric variables which exhibit a strong signature in the high intensity cells, the behaviour of Ψ_{dp} is of particular interest. In the areas characterized by high Z_{dr}, the presence of large positive bumps are associated with the differential phase shift on backscattering δ (see Figure 5). From a visual inspection, values of δ on the order of 20-25° are evident. In order to obtain a quantitative estimation, a simple procedure was applied, as described in Chapter 3. It is interesting to note that the copolar correlation coefficient ρ_{hv} drops to values around 0.95 and in some cases even below 0.9, in correspondence to the peaks of Z_{dr} (and δ).

3 Measurement interpretation

The interpretation of the event under investigation, in terms of microphysical processes occurring, is not straightforward, and two possible explanations have been considered. In convective cases, liquid precipitation can be mixed with solid phase, and the goal here is to understand which is the dominant process among liquid and ice-phase precipitation, leading to such high polarimetric signature. The following sections detail each explanation.

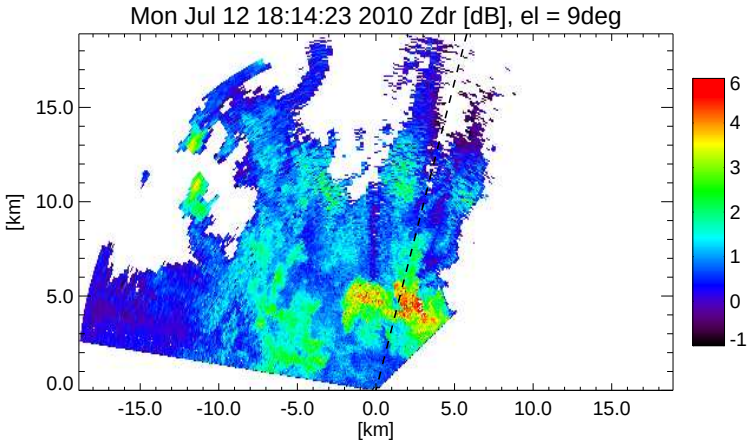

Figure 3: *Same as Figure 1, for the differential reflectivity Z_{dr}.*

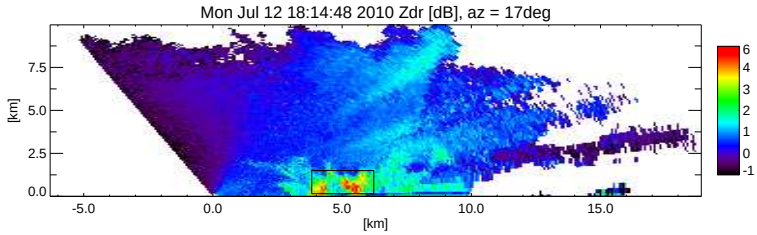

Figure 4: *Same as Figure 2, for the differential reflectivity Z_{dr}.*

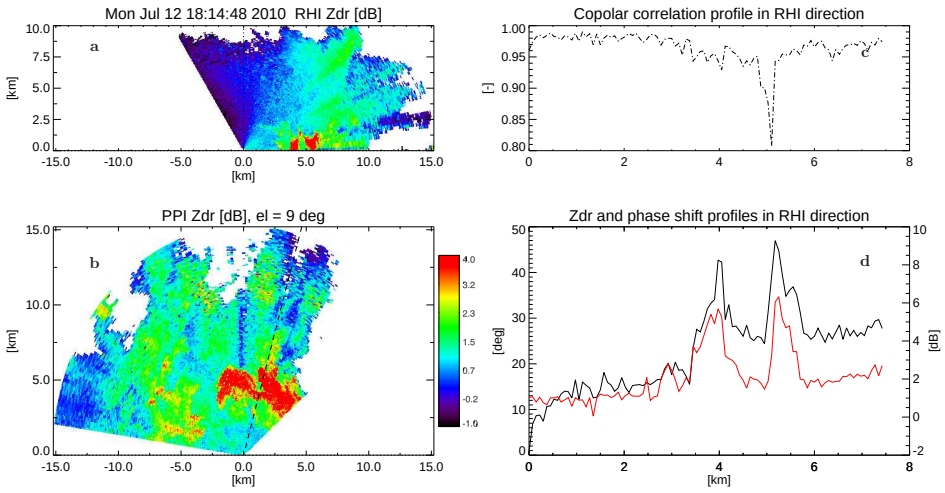

Figure 5: *(a): RHI of Z_{dr} (1814 UTC); (b): PPI of Z_{dr} (1814 UTC) at an elevation of 9°, the dotted line shows the direction of the RHI scan. (c): Range profile of ρ_{hv} extracted from the RHI scan, at an elevation of 3°. (d): Corresponding range profiles of Z_{dr} (red) and Ψ_{dp} (black). For the panels (a) and (b), the colorscale has been set to a maximum of 4 dB and saturated in order to better highlight the high intensity areas.*

3.1 Rainfall influenced by large drops

As we can see in Figures 4 and 5, the intense part of the convective cells are evident as column of positive and high Z_{dr}, which are mainly confined below the estimated melting region. The melting region is located approximately at an altitude of 2 km above the radar, and it becomes evident in the later stage of the event, when the convection is replaced by a stratiform configuration. Positive column of Z_{dr} in rain have been described in Hall et al. (1984) and Bringi and Chandrasekar (2001). In such cases, the measurements were associated

with the effect of updraft, leading to the coalescence of drops and to the formation of large (more than 6 mm) and oblate drops. The effect of these drops, even if in relatively small concentration, can be large on shape-dependent parameters like Z_{dr}. The effect in terms of differential phase shift on backscattering was not quantified in the mentioned studies. High values of δ can be observed at short wavelengths, and a well defined power-law relation between δ and Z_{dr} emerges, resulting in expressions of the form $\delta = aZ_{dr}^b$. The parameter b has found to be 1.8 at X-band (Otto and Russchenberg, 2011). From our independent scattering calculations on simulated DSD fields the parameter b is about 1.8, confirming the robustness of the relation.

In order to verify that the areas of enhanced polarimetric signatures are dominated by rain, we proceed as follows. Using the RHI scans from 1800 UTC to 1900 UTC, we could track the main cell while it is moving from the South to the North. A rectangular sub-domain, with a width of 2400 m and an height of 900 m (Figure 2) is moved horizontaly at each time step, in order to fully include the high intensity cores of Z_h and Z_{dr}. The chosen vertical extension is motivated by the willingness to focus our analysis on areas assumed to be below the freezing level and to avoid including regions where the excessive elevation of the incident beam has direct geometrical consequences on the behaviour of Z_h and Z_v. On the subdomain defined in this way, the values of the polarimetric variables have been extracted. In addition, the reflectivity difference Z_{dp} [dBZ] has been calculated as:

$$Z_{dp} = 10 \log_{10} (Z_h - Z_v) \tag{1}$$

with $Z_{h,v}$ in linear units [mm^6 m^{-3}]. Z_{dp} in rain is usually highly correlated with Z_h [dBZ], and the correlation coefficient between them tends to unity (Bringi and Chandrasekar, 2001). In case of significant presence of ice-phase hydrometeors, the correlation is lower, and some values of Z_h exceed Z_{dp} significantly, and are situated on the right side of a $Z_h - Z_{dp}$ plot. In our case, the correlation between Z_h and Z_{dp} is very strong ($R = 0.992$), and only a limited number of points slightly exhibit the behaviour of ice (Figure 6(a)). This substantially means that the precipitation in the cells analyzed behaves mostly like rain.

An experimental investigation of the high values of δ, and their relation with Z_{dr} values is then carried out, in the mentioned subdomains. The estimation of δ is known to be noisy (Otto and Russchenberg, 2011), but in such a strong case, it is assumed that we are able to isolate at least its highest values with sufficient accuracy. δ is estimated by subtraction of Ψ_{dp} and Φ_{dp} profiles, once Φ_{dp} has been obtained by iterative filtering of Ψ_{dp} profiles, but in this case the filter has been selected to be more aggressive compared to what is described by Hubbert and Bringi (1995), and usually applied in conventional MXPol data processing. The goal here is not to preserve the small-scale variations of Φ_{dp}, for subsequent K_{dp} estimation, but to isolate the significant contribution of δ. A scatterplot of Z_{dr} and δ values has been constructed and an experimental fit took the form of $\delta = 0.4Z_{dr}^2$ which is reasonably close, given the dispersion of the values, to the estimation derived by scattering simulations. It must be noted that, in this case, it is experimentally extended to a wider range of δ-Z_{dr} values (Figure 6(b)).

Furthermore, to evaluate if the polarimetric signature could be effectively associated with the presence of large drops, the data collected by the Parsivel disdrometers deployed in Davos (locations indicated in Figure 1) are used. Even if the stations were only partially affected by the most intense cells, one station was positioned in an area sufficiently close to a cell core (Z_{dr} about 3.5 dB) from 1800 UTC to 1810 UTC. The volumic DSD is used to construct a time series of Z_{dr}, using the T-matrix scattering simulation approach (Mishchenko et al., 1996) and the drop shape model from Andsager et al. (1999). The time series are calculated for (i) complete measured DSD and (ii), for the DSD truncated at 6 mm. As we can observe in Figure 7(a), the truncated distribution leads to a significant reduction in Z_{dr} peaks, and this happens only in the period interested by the edge of the convective cell. This is an indication of the presence of large particles in a significant (in terms of Z_{dr} effect) concentration.

A last point to be evaluated is whether a consistent updraft is indeed present. As a preliminary step, the small-scale change in the mean radial velocity around the cells (see Figure 7(b)) are interpreted as the signature of strong turbulence that could be associated with updraft. Further analysis are necessary to clarify the flow patterns in the vicinity of the cells.

3.2 Precipitation in form of hail

A second interpretation of the event under investigation is to consider the presence of hail. The classical interpretation (Herzegh and Jameson, 1992; Depue et al., 2007) assumes that the tumbling of hail causes a loss of preferential orientation, and therefore leads to values of Z_{dr} close to 0. From Smyth et al. (1999) observations was showed how oblate hail can lead to positive Z_{dr} values even if the reasons and the description of a non-tumbling falling mode are still an open question for the scientific community. Furthermore, wet melting hail, from theoretical computations (Aydin and Zhao, 1990) can lead, at X-band, to large Z_{dr} values and to an important decrease of ρ_{hv}, even below 0.9. This seems in agreement with our measurements, as shown in Figure 5. It is in fact difficult to explain such an important decrease of ρ_{hv} in rain even in presence of strong

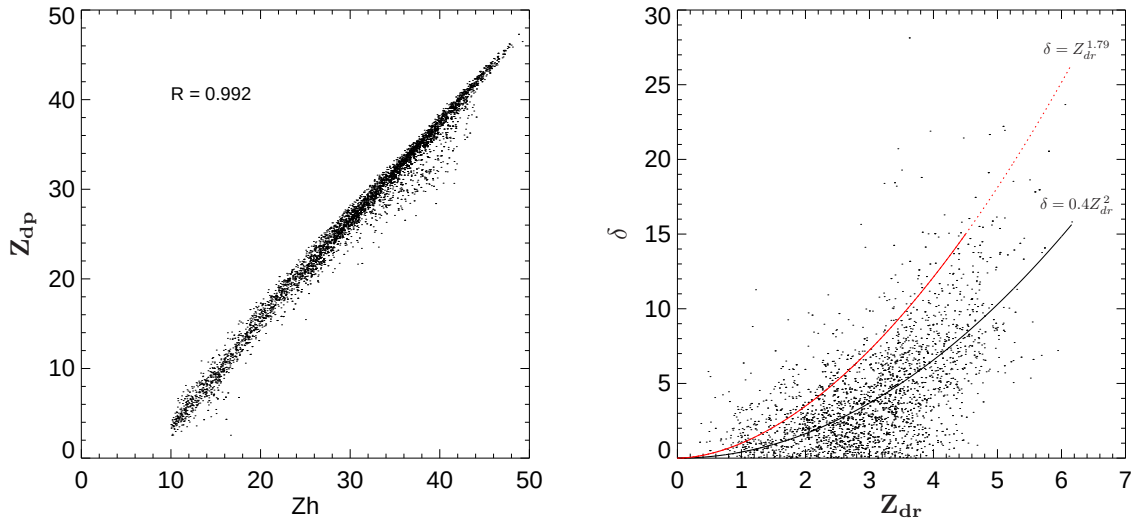

(a) (b)

Figure 6: *(a): Scatterplot and correlation coefficient R between Z_{dp} and Z_h in a moving window designed to track the most intense convective cell, moving in the RHI direction from 1750 UTC to 1900 UTC. (b): Scatterplot of Z_{dr} and δ values obtained in the same region. The red line indicates the theoretical power law relation between the polarimetric quantities, and the dotted part represents the extrapolation outside the range of Z_{dr} obtained in the simulations. The black line shows the same power-law calculated for the measured data.*

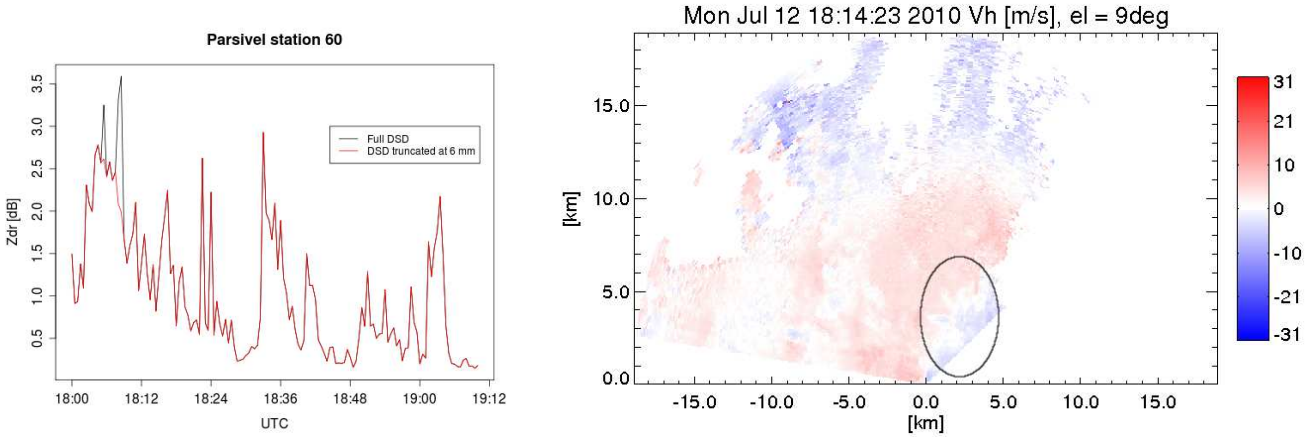

(a) (b)

Figure 7: *(a): Time series of Z_{dr} values calculated using DSD data from a Parsivel disdrometer. The black line indicates the time series, when the full DSD is used, while the red line uses DSD truncated at a D_{max} of 6 mm. (b) PPI of Mean Doppler velocity (1814 UTC). Note the area, correspondent to the strong cell of Figure 1, where the velocity changes its sign.*

attenuation. Most important, always according to Aydin and Zhao (1990), melting hail may lead to large positive values of δ.

Another typical feature of hail, used in hail detection schemes since Waldvogel et al. (1979) is the presence of high values of Z_h in areas at least 1.4 km above the melting layer. The threshold proposed at that time was of 45 dBZ (for S-band). Taking this information qualitatively, we can effectively observe areas of relatively high Z_h, at a considerable height. They are visible in Figure 2, and also in previous time-steps.

4 Conclusions and future work

X-band observations of a convective event characterized by cells of high positive values of Z_{dr} and δ has been presented. The extraordinary aspect of the case raised questions about the microphysical processes occurring in such cells. Two possible explanations in terms of dominant processes has been found. In the first, the dominant process is supposed to be updrafted rain, leading to an unusual concentration of large oblate drops in liquid phase. This was leading to an investigation of the relations between polarimetric variables in the high intensity cells, with a particular focus on the values of Z_{dr} and δ. A second explanation, supported by theoretical studies and previous observations is related to the presence of oblate hail falling with a preferential orientation. At this stage of our investigation it is difficult to select one or the other. In both cases, the data presented in this contribution will experimentally confirm and extend previous work mainly based on scattering simulations.

Future work will involve the investigation of updraft forces, and an attempt to quantify them using the available Doppler information. Furthermore, precise ground reports on the possible presence of hail in correspondence of the cells have to be found.

Acknowledgements

This work is funded by the Swiss National Science Fundation under Grant 200021-125064. Significant further funding has been obtained from the Competence Center of Environment and Sustainability (CCES) of the ETH domain through the Swiss-Experiment Project. The authors also thank Marc Schneebeli and Joel Jaffrain (LTE) for the collection of data.

References

Andsager, K., K. V. Beard, and N. F. Laird, 1999: Laboratory measurements of axis ratios for large rain drops. *J. Atmos. Sci.*, **56 (15)**, 2673–2683.

Aydin, K. and Y. Zhao, 1990: A computational study of polarimetric radar observables in hail. *IEEE T. Geosci. Remote Sens.*, **28 (4)**, 412–422, doi:10.1109/TGRS.1990.572906.

Beard, K. V., V. N. Bringi, and M. Thurai, 2010: A new understanding of raindrop shape. *Atmos. Res.*, **97 (4)**, 396–415, doi:10.1016/j.atmosres.2010.02.001.

Bringi, V. N. and V. Chandrasekar, 2001: *Polarimetric doppler weather radar*. Cambridge University Press, 662 pp.

Depue, T. K., P. C. Kennedy, and S. A. Rutledge, 2007: Performance of the hail differential reflectivity (hdr) polarimetric radar hail indicator. *J. Appl. Meteor. Climate*, **46 (8)**, 1290–1301, doi:10.1175/JAM2529.1.

Hall, M. P. M., J. W. F. Goddard, and S. M. Cherry, 1984: Identification of hydrometeors and other targets by dual-polarization radar. *Radio Sci.*, **19**, 132–140.

Herzegh, P. and A. Jameson, 1992: Observing precipitation through dual-polarization radar measurements. *Bull. Amer. Meteor. Soc.*, **73 (9)**, 1365–1374, doi:10.1175/1520-0477(1992)073¡1365:OPTDPR¿2.0.CO;2.

Hubbert, J. and V. N. Bringi, 1995: An iterative technique filtering technique for the analysis of copolar differential phase and dual-frequency polarimetric variables. *J. Atmos. Oceanic Technol.*, **12 (3)**, 643–648.

Mishchenko, M. I., L. D. Travis, and D. W. Mackowski, 1996: T-matrix computations of light scattering by nonspherical particles: A review. *J. Quant. Spectrosc. Radiat. Transfer*, **55 (5)**, 535–575.

Otto, T. and H. W. J. Russchenberg, 2011: Estimation of Specific Differential Phase and Differential Backscatter Phase From Polarimetric Weather Radar Measurements of Rain. *IEEE Geosci. Remote Sens. Lett.*, **8 (5)**, 988–992.

Schleiss, M., J. Jaffrain, and A. Berne, 2012: Stochastic simulation of intermittent DSD fields in time. *J. Hydrometeor.*, **13 (2)**, 621–637, doi:10.1175/JHM-D-11-018.1.

Smyth, T., T. Blackman, and A. Illingworth, 1999: Observations of oblate hail using dual polarization radar and implications for hail-detection schemes. *Q. J. Roy. Meteor. Soc.*, **125 (555)**, 993–1016, doi:10.1256/smsqj.55511.

Testud, J., E. Le Bouar, E. Obligis, and M. Ali-Mehenni, 2000: The rain profiling algorithm applied to polarimetric weather radar. *J. Atmos. Oceanic Technol.*, **17 (3)**, 332–356.

Thurai, M., D. Hudak, and V. N. Bringi, 2008: On the possible use of copolar correlation coefficient for improving the drop size distribution estimates at c band. *J. Atmos. Oceanic Technol.*, **25 (10)**, 1873–1880.

Waldvogel, A., B. Federer, and P. Grimm, 1979: Criteria for the detection of hail cells. *J. Appl. Meteor.*, **18 (12)**, 1521–1525.

Wang, Y. T. and V. Chandrasekar, 2009: Algorithm for estimation of the specific differential phase. *J. Atmos. Oceanic Technol.*, **26 (12)**, 2565–2578, doi:10.1175/2009JTECHA1358.1.